SCIENTIFIC REPORTS

OPEN

SUBJECT AREAS:
CALCIUM SIGNALLING
HEART FAILURE
MUSCLE CONTRACTION
PHOSPHORYLATION

Received
13 February 2013

Accepted
22 May 2013

Published
12 June 2013

Correspondence and requests for materials should be addressed to M.V.W. (wfall@umich.edu)

* Current address: Dept. of Physiology Medical Research Building 320 University of Arizona College of Medicine Tucson, AZ 85724.

Agonist Activated PKCβII Translocation and Modulation of Cardiac Myocyte Contractile Function

Hyosook Hwang[1]*, Dustin Robinson[1], Julie B. Rogers[1], Tamara K. Stevenson[1], Sarah E. Lang[2], Sakthivel Sadayappan[3], Sharlene M. Day[4], Sivaraj Sivaramakrishnan[5] & Margaret V. Westfall[1,2]

[1]Department of Cardiac Surgery, University of Michigan, Ann Arbor, MI 48109, [2]Program in Cellular and Molecular Biology, University of Michigan, Ann Arbor, MI 48109, [3]Department of Physiology, Loyola University of Chicago, Maywood, IL 60153, [4]Cardiovascular Division, Department of Internal Medicine, University of Michigan, Ann Arbor, MI 48109, [5]Department of Cellular and Developmental Biology, University of Michigan, Ann Arbor, MI 48109.

Elevated protein kinase C β_{II} ($PKC\beta_{II}$) expression develops during heart failure and yet the role of this isoform in modulating contractile function remains controversial. The present study examines the impact of agonist-induced $PKC\beta_{II}$ activation on contractile function in adult cardiac myocytes. Diminished contractile function develops in response to low dose phenylephrine (PHE, 100 nM) in controls, while function is preserved in response to PHE in $PKC\beta_{II}$-expressing myocytes. PHE also caused $PKC\beta_{II}$ translocation and a punctate distribution pattern in myocytes expressing this isoform. The preserved contractile function and translocation responses to PHE are blocked by the inhibitor, LY379196 (30 nM) in $PKC\beta_{II}$-expressing myocytes. Further analysis showed downstream protein kinase D (PKD) phosphorylation and phosphatase activation are associated with the LY379196-sensitive contractile response. PHE also triggered a complex pattern of end-target phosphorylation in $PKC\beta_{II}$-expressing myocytes. These patterns are consistent with bifurcated activation of downstream signaling activity by $PKC\beta_{II}$.

Classical PKC up-regulation has been linked to human and animal models of heart failure for over a decade[1–3]. Cardiac dysfunction is associated with up-regulation of PKCα, $PKC\beta_I$ and/or $PKC\beta_{II}$ classical isoforms in response to pressure overload, ischemia, and inherited mutations[1,4–6]. Under physiological conditions, PKCα is the major classical isoform expressed in adult mammalian hearts and it negatively modulates contractile function[7–9]. In mouse models, up-regulation of PKCα targets phosphorylation of inhibitor 1 (I-1), which then activates protein phosphatase I (PP1) activity, and in turn de-phosphorylates proteins such as phospholamban to diminish cardiac performance[10]. While there is substantial work devoted to understanding the role played by up-regulation of $PKC\beta_{II}$ during heart failure[2,11–15], the contribution of this isozyme to cardiac dysfunction and heart failure remains controversial.

Genetic models often provide insight into the role played by a specific kinase, but this has not been the case for $PKC\beta_{II}$. Cardiac specific transgenic expression of wildtype $PKC\beta_{II}$ produced a loss of function phenotype[3,15], while inducible, cardiac-specific expression of constitutively active $PKC\beta_{II}$ improved contractile function[12]. More recently, pharmacologic treatments targeting PKCβ as well as work in knockout models produced equally divergent ideas about the role of $PKC\beta_{II}$ during heart failure[5,7,14]. An integrative approach utilizing animal models is ultimately necessary to understand the role of kinases such as $PKC\beta_{II}$ in complex disease states, such as heart failure. However, studies in isolated myocytes may provide important insights into the role $PKC\beta_{II}$ plays in modulating contractile function and help resolve the controversy about the impact of $PKC\beta_{II}$ on myocyte contractile function.

In a recent report, up-regulated wildtype $PKC\beta_{II}$ was localized in a peri-nuclear distribution pattern under basal conditions and produced diminished contractile function within 2 days after gene transfer[16]. This decrease in function was associated with alterations in Ca^{2+} handling and a complex phosphorylation response in downstream Ca^{2+} handling and myofilament proteins. The present study extends this work to determine whether known PKC agonists activate and re-distribute $PKC\beta_{II}$ and change contractile function after vector-mediated $PKC\beta_{II}$ gene transfer and expression in isolated rat cardiac myocytes. The divergent phenotypic responses reported in different genetic animal models led to the hypothesis that basal and agonist stimulation may produce different $PKC\beta_{II}$ localization patterns and functional responses in adult myocytes. The present study focuses on

the contractile function response to low doses of phenylephrine (PHE) to initially test this idea. In addition, the functional responses to moderate PHE doses, as well as phorbol 12-myristate 13-acetate (PMA), and endothelin-1 (ET-1) also are examined in this study. In contrast to the recently reported decrease in basal function[16], agonist-mediated activation is anticipated to enhance function in myocytes. This prediction is based on the functional improvements reported in mice expressing an inducible, constitutively active $PKC\beta_{II}$[12].

Downstream signaling also is examined in parallel experiments to determine whether changes in target protein phosphorylation levels are associated with the functional response. The results indicate $PKC\beta_{II}$ activation by low dose PHE preserves myocyte contractile function, and produces a complex signaling response. A bifurcated downstream signaling pathway may help explain this complex signaling pathway in animal models.

Results

Experiments in this study examined the influence of $PKC\beta_{II}$ up-regulation on agonist-mediated contractile function in cardiac myocytes. These functional studies were performed with adult rat cardiac myocytes 2 days after gene transfer, which is a time point when $PKC\beta_{II}$ up-regulation (Fig. 1A) was similar to the increase observed in failing human hearts[16]. The reduction in basal shortening associated with elevated $PKC\beta_{II}$ expression prior to agonist delivery (Fig. 2A) also was consistent with earlier results[16].

Agonist-induced contractile function response. The contractile function response to 100 nM PHE was examined in control, $PKC\beta_{II}$-, and PKCβDN-expressing myocytes to determine whether agonist-activation of $PKC\beta_{II}$ produces a specific functional response. During 15 min perfusion with PHE, the amplitude and rates of shortening and re-lengthening were preserved and/or slightly increased in $PKC\beta_{II}$-expressing myocytes (Fig. 1B, 2B,C). In contrast, the shortening amplitude decreased and the rates of shortening and re-lengthening slowed in control and PKCβDN-expressing myocytes. Addition of the PKCβ inhibitor, LY379196 (LY) to $PKC\beta_{II}$-expressing myoyctes restored PHE-induced decreases in contractile function, without influencing the responses of control or PKCβDN-expressing myocytes (Fig. 1B,2D). This preservation of contractile function in response to PHE also was observed 3 days after gene transfer in $PKC\beta_{II}$-expressing myocytes (Fig. 2E). However, a differential response between control and $PKC\beta_{II}$-expressing myocytes was not detected with 1 μM PHE (Fig. 3B,C) or with PMA (50 nM; Fig. 3D,E).

PHE-mediated $PKC\beta_{II}$ phoshorylation, localization and distribution. Phosphorylation and localization of $PKC\beta_{II}$ were examined to begin analyzing events contributing to the divergent functional response to 100 nM PHE. In control myocytes, PKC αThr638/β641 phosphorylation increased in response to PHE (Fig. 4A), presumably due to increases in PKCα phosphorylation. In myocytes expressing $PKC\beta_{II}$, the enhanced phosphorylation of classical PKCs detected under basal conditions[16] is not further increased by 100 nM PHE (Fig. 4A). The relative contribution of phosphorylated PKCα versus β_{II} during the PHE response remains unclear based on these results.

In addition, classical PKC phosphorylation in response to agonists is linked to kinase activation and translocation[17]. Thus, immunohistochemical (IHC) labeling and fractionation were used to determine whether 100 nM PHE induces $PKC\beta_{II}$ translocation. Treatment with 100 nM PHE caused the basal, peri-nuclear distribution of $PKC\beta_{II}$[16] to transition to a striated pattern within 10 min of incubating myocytes in PHE (Fig. 4B). This PHE-induced shift in $PKC\beta_{II}$ localization is similar to the striated distribution of α-actinin in the myofilament, and indeed these patterns overlapped in merged images. On close examination, the striated $PKC\beta_{II}$ fluorescence is more uneven or punctate than the α-actinin pattern. This pattern resembles the more punctate t-tubule distribution of transporters such as the Na^+/Ca^{2+} exchanger[18] (NCX). The LY antagonist prevented the PHE-induced translocation, and the $PKC\beta_{II}$ distribution pattern remained similar to the peri-nuclear pattern observed under basal conditions (Fig. 4C).

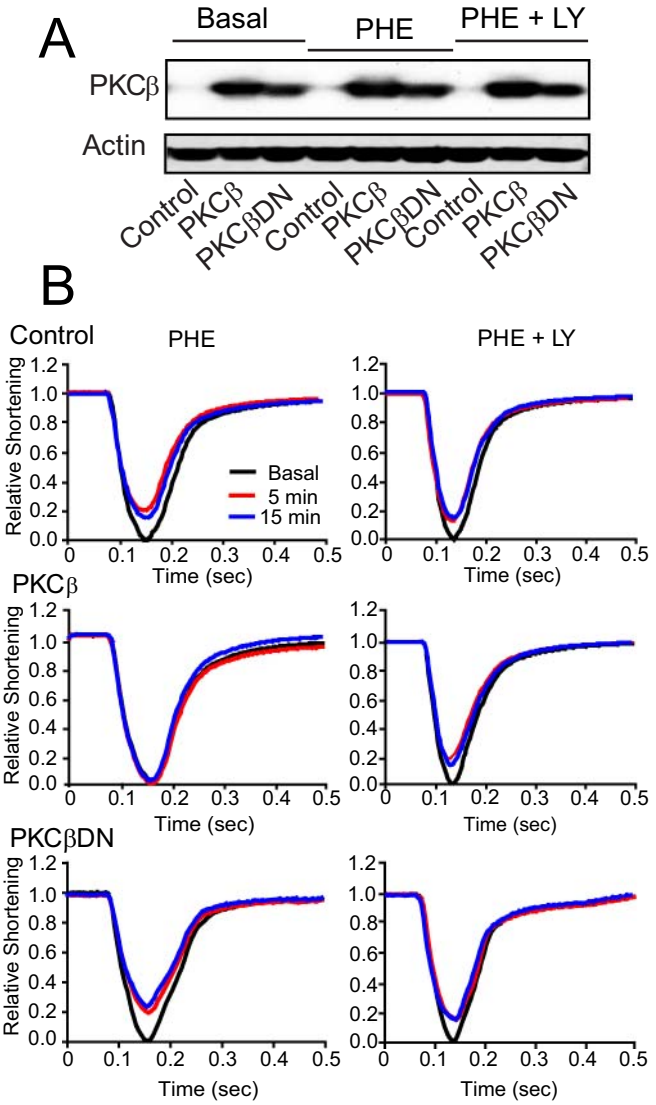

Figure 1 | Adult cardiac myocyte $PKC\beta_{II}$ and PKCβDN expression and contractile function in response to phenylephrine (PHE; 100 nM) or PHE plus the PKCβ inhibitor, LY379196 (LY, 30 nM). (A). Representative Western blot of PKCβ and PKCβDN expression 2 days after gene transfer compared to non-treated controls. Protein expression is shown under basal conditions (left), in the presence of 100 nM PHE (10 min, middle) and PHE plus LY (10 min, right). (B). Composite shortening traces collected under basal conditions and then 5 and 15 min after the addition of PHE in the absence (left panels) and presence (right panels) of the PKCβ inhibitor, LY. The PHE-induced decrease in shortening amplitude observed in controls (upper left panel; n = 19) and PKCβDN-expressing myocytes (lower left panel; n = 13) is absent in $PKC\beta_{II}$-expressing (middle left panel, n = 16) myocytes. In $PKC\beta_{II}$-expressing myocytes (middle right panel; n = 24), the addition of LY379196 with PHE returns the response to the control pattern observed with PHE. LY does not change the PHE-induced shortening response in control (upper right panel; n = 28) or PKCβDN-expressing myocytes (lower right panel; n = 13). Quantitative analysis of contractile function measured before and after PHE or PHE+LY treatment is summarized in Figure 2.

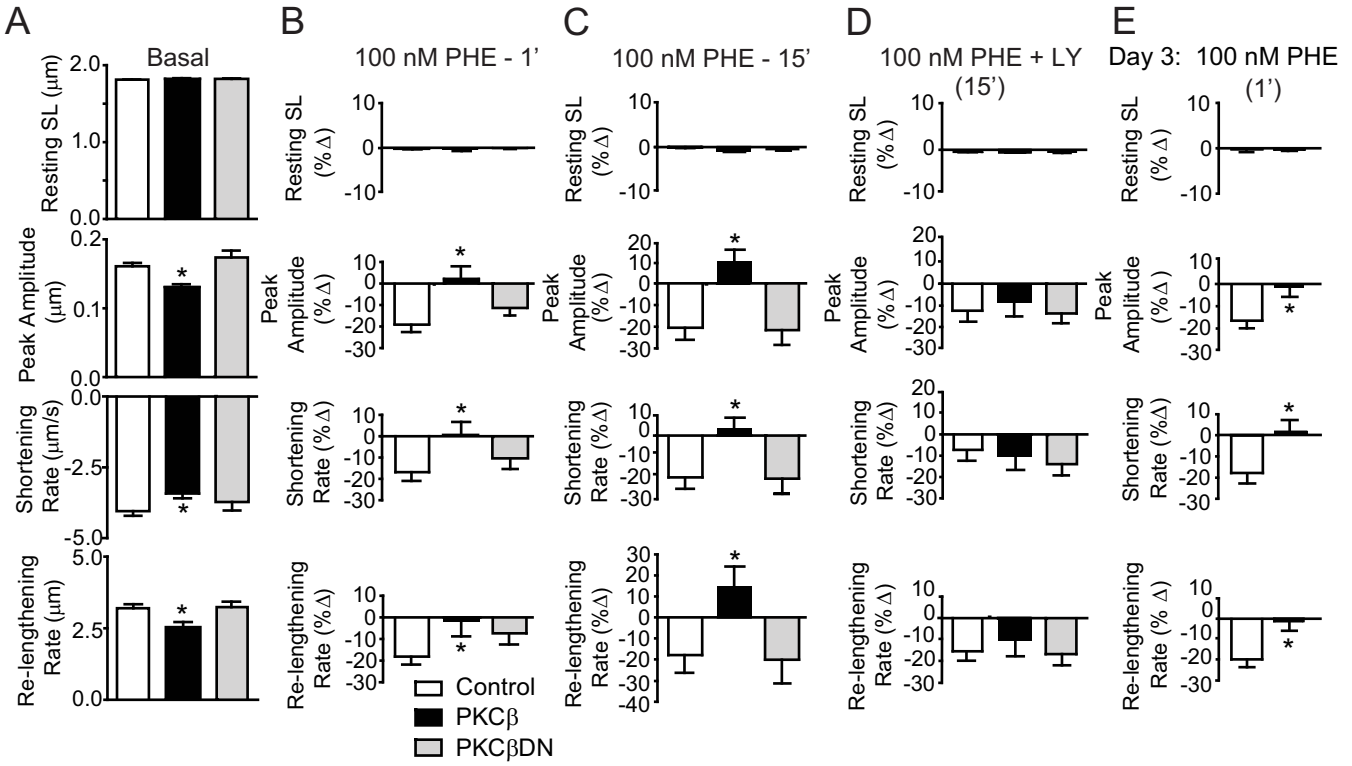

Figure 2 | Quantitative analysis of contractile function under basal conditions and in response to PHE or PHE+LY in control, PKCβ$_{II}$-, and PKCβDN-expressing myocytes. (A). Analysis of basal function in the control (n = 46), PKCβ$_{II}$-(n = 40), and PKCβDN- (n = 26) expressing myocytes used for the subsequent analysis of PHE and PHE+LY responses (panels B–D). Basal values and the PKCβ$_{II}$-induced decreases in shortening and re-lengthening are comparable to values reported in earlier work (16). The response to PHE and PHE+LY is expressed as a percent change (% Δ) from basal values in the remaining panels (B–E). PHE-induced changes in myocyte shortening and re-lengthening were analyzed 1 (B) and 15 (C) min (Control n = 18; PKCβ$_{II}$ n = 16; PKCβDN n = 13) after PHE, and 15 min after addition of PHE plus LY (D; Control n = 28; PKCβ$_{II}$ n = 24; PKCβDN n = 13) 2 days after gene transfer. The response to PHE 3 days after gene transfer is shown in (E) (Control n = 15; PKCβ$_{II}$ n = 16) to demonstrate the consistency of this response in myocytes expressing PKCβ$_{II}$ relative to controls. Differences in function are identified using a one-way ANOVA and Newman-Keuls post-hoc tests, with $p < 0.05$ (*) considered significantly different from control values in the present figure and in Figure 3.

The PKCβ$_{II}$ distribution pattern in response to PHE also was studied after fractionation. Most PKCβ$_{II}$ resided in the cytosol under basal conditions. This isoform transitioned into the myofilament fraction in response to PHE and LY attenuated this translocation (Fig. 4D). While the membrane fraction is enriched in sarcolemmal proteins, t-tubule and junctional sarcoplasmic reticulum proteins also are found in the myofilament fraction[19]. PKCβ$_{II}$ also tended to move into the membrane fraction during the PHE response, although the increase and inhibition by LY were not statistically significant. Overall, the IHC and fractionation studies indicate low dose PHE activates PKCβ$_{II}$ translocation over the same time interval as the PKCβ-specific functional response.

Western analysis of downstream kinases. In earlier work, PKCβ$_{II}$ up-regulation significantly increased Ca^{2+}/calmodulin protein kinase IIδ (CaMKIIδ) Ser286 and protein kinase D (PKD) Ser744/748 phosphorylation under basal conditions[16]. CaMKIIδ and PKD phosphorylation were studied here to determine whether PKCβ$_{II}$ also targets these downstream kinases during the low dose PHE response. PHE did not influence CaMKIIδ phosphorylation in controls and PKCβDN-expressing myocytes, and did not further enhance the phosphorylation of this kinase observed under basal conditions in PKCβ$_{II}$-expressing myocytes (Fig. 5A). The comparable level of CaMKIIδ phosphorylation under basal conditions and in response to PHE for controls and PKCβDN-expressing myocytes is in agreement with our earlier work[16]. As reported previously, addition of LY also did not change pCaMKIIδ phosphorylation in response to PHE in PKCβ$_{II}$-expressing myocytes (results not shown). These results indicate this low dose PHE does not alter PKCβ$_{II}$ targeting of CamKIIδ. However, addition of the phosphatase inhibitor, calyculin A (calA) along with PHE further increased CamKIIδ phosphorylation compared to PHE alone in myocytes expressing PKCβ$_{II}$ (Fig. 5A), which was attenuated by LY (Supp Figure 1A). In contrast, CaMKIIδ phosphorylation remained nearly undetectable in response to calA and LY in controls and PKCβDN-expressing myocytes. These results suggest PKCβ$_{II}$ activation by PHE accelerates CaMKIIδ phosphorylation turnover during the PHE response.

In contrast to CamKIIδ, PKD phosphorylation increased in response to low dose PHE in controls and myocytes expressing PKCβ$_{II}$ or PKCβDN (Fig. 5B). Myocytes expressing PKCβ$_{II}$ developed the highest levels of PKD phosphorylation during the PHE response, and this increase was attenuated by LY (Fig. 5C). In contrast, the enhanced PKD phosphorylation produced by 100 nM PHE was not changed by the inhibitor in control and PKCβDN-expressing myocytes. To determine whether PHE influences phosphorylation turnover on PKD, experiments were carried out in the presence of the calA phosphatase inhibitor and with the protein kinase A (PKA) inhibitor, PKI. PKA activation of phosphodiesterases could influence phosphorylation turnover[20], but PKI inhibition of PKA did not change the PHE-mediated enhancement of PKD phosphorylation (Fig. 5D). Addition of the phosphatase inhibitor calA along with PHE also produced a comparable level of PKD phosphorylation as PHE plus PKI in all 3 groups (results not shown). However, PKD phosphorylation was partially attenuated when LY was added along with PHE plus calA in PKCβ$_{II}$-expressing myocytes. The addition of

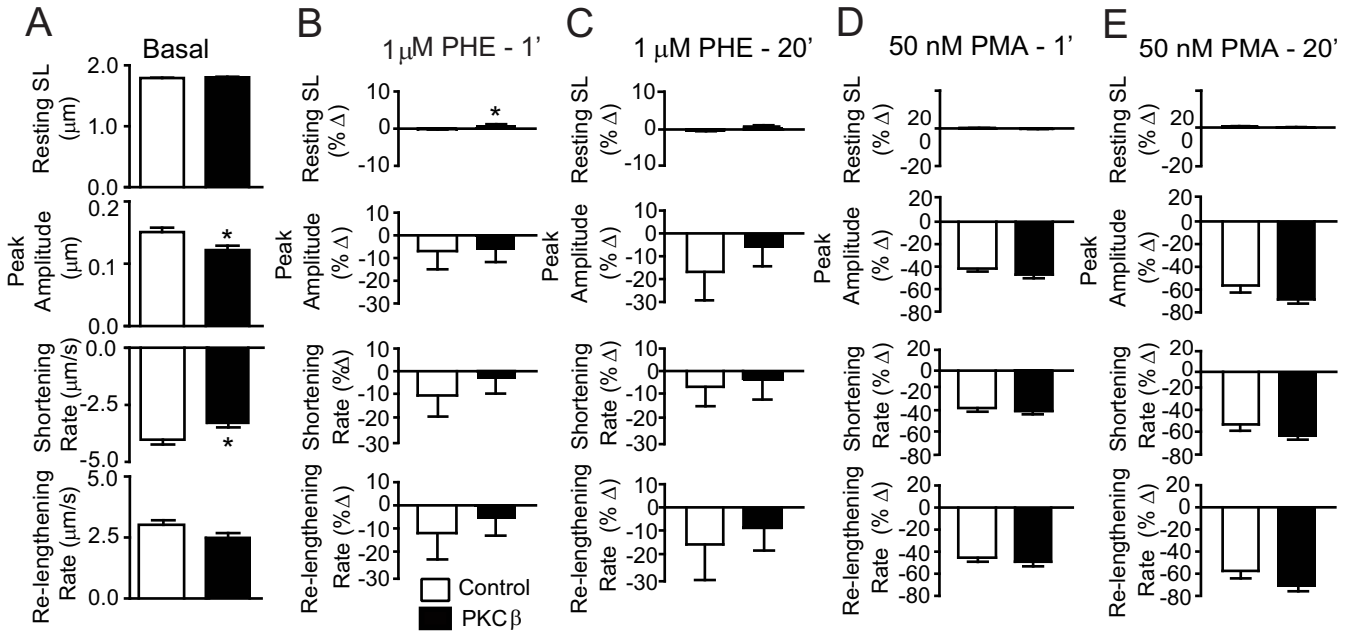

Figure 3 | Quantitative analysis of basal contractile function before 1 μM PHE or 50 nM phorbol 12,13 myristic acid (PMA) (A; Control n = 39, PKCβ$_{II}$ n = 35), and in response to 1 (B, D) and 20 (C, E) min of 1 μM PHE (B, C; Control n = 12; PKCβ$_{II}$ n = 10) or 50 nM PMA (D, E; Control n = 27; PKCβ$_{II}$ n = 25) in control and PKCβ$_{II}$-expressing myocytes. Agonist-induced decreases in shortening amplitude, and shortening and re-lengthening rates were not different in control and PKCβ$_{II}$-expressing myocytes in response to 1 μM PHE (B, C). Comparable decreases in the rates and amplitude of shortening and re-lengthening also were observed in control and PKCβ$_{II}$-expressing myocytes after 1 (D) and 20 (E) min of 50 nM PMA.

LY did not change the response to PHE plus calA in controls or PKCβDN-expressing myocytes. This attenuated PKD phosphorylation response to PHE in PKCβ$_{II}$-expressing myocytes also resulted in no difference in PKD phosphorylation compared to PKCβDN-expressing and control myocytes (Fig. 5D). Together, these studies show low dose PHE causes PKCβ$_{II}$ to phosphorylate and presumably activate PKD, which could contribute to the divergent functional responses observed in PKCβ$_{II}$ versus control myocytes.

Western analysis of myofilament and Ca^{2+} cycling protein targets. Our work then focused on potential myofilament protein targets for the PKCβ$_{II}$–dependent component of the PHE response based on the temporal association between myocyte contractile function, striated PKCβ$_{II}$ localization, and downstream PKD phosphorylation in PKCβ$_{II}$-expressing myocytes. In ^{32}P radiolabeling experiments, PHE increased myosin light chain 2 (MLC_2), cTnI, and cMyBP-C phosphorylation above basal levels in PKCβ$_{II}$-expressing myocytes compared to controls, and LY attenuated these increases without influencing phosphorylation in control myocytes (Fig. 6A). Phosphorylation of cTnI and cMyBP-C also is enhanced in PKCβ$_{II}$-expressing myocytes under basal conditions (Fig. 6A, ref. 16), and both PKC and PKD target these proteins[21,22]. Further analysis of the PKD-responsive residues on cTnI (e.g. Ser23/24; Fig. 6) and cMyBP-C (Ser302; Fig. 7) in addition to the cMyBP-C Ser273 and Ser282 sites were examined with phospho-specific antibodies. Western blot analysis indicated PHE had little influence on cTnI Ser23/24 phosphorylation in control myocytes, and phosphorylation of these residues in PKCβ$_{II}$-expressing myocytes was similar to controls during low dose PHE (Fig. 6B). The increased cTnI phosphorylation detected in PKCβ$_{II}$-expressing myocytes during the low dose PHE response in the radiolabeling experiment and lack of change detected at Ser23/24 could indicate alternate residues on cTnI are phosphorylated by the PKCβ$_{II}$ pathway. The more likely explanation is the presence of a phosphatase inhibitor in radiolabeling studies (Fig. 6A) but not in the Western analysis (Fig. 6B). This later possibility was confirmed with the addition of calA during the PHE response, which resulted in elevated cTnISer23/24 phosphorylation in PKCβ$_{II}$-expressing myocytes (Fig. 6C,E). An unexpected finding was the further enhancement of PHE-induced cTnISer23/24 phosphorylation with the addition of LY in myocytes expressing PKCβ$_{II}$ compared to controls or PKCβDN-expressing myocytes (Fig. 6D,E). The influence of LY is consistent with PKCβ$_{II}$ targeting both phosphatase and PKD activity, and low dose PHE causing PKCβ$_{II}$ to target phosphatase over kinase activation in the absence of a phosphatase inhibitor. In studies with PMA, the cTnISer23/24 phosphorylation response to this PKC activator was similar in control and PKCβ$_{II}$-expressing myocytes (Fig. 6F).

Myocytes expressing PKCβ$_{II}$ also develop enhanced cMyBP-C phosphorylation[16], and PHE produced a unique pattern of Ser273, Ser282 and Ser302 phosphorylation in these myocytes (Fig. 7). Cardiac MyBP-C Ser282 phosphorylation (p282) tended to decrease with PHE in PKCβ$_{II}$-expressing myocytes relative to controls and LY attenuated this change (Fig. 7A,B). The trend toward decreased pSer282 in response to PHE also was attenuated when calyculin A was included with PHE (Supp Figure 1B). These trends are consistent with dual downstream kinase and phosphatase modulation by PKCβ$_{II}$ activation during the PHE response. In contrast, cMyBP-C Ser273 and Ser302 phosphorylation were not substantially changed by PHE in control, PKCβ$_{II}$ or PKCβDN-expressing myocytes compared to basal values. Phosphorylation of cMyBP-C Ser273 was not detected under basal conditions or in response to PHE in any of the 3 myocyte groups (results not shown). The enhanced basal phosphorylation of Ser302 in PKCβ$_{II}$-expressing myocytes (Fig. 7A; ref. 16) was not further elevated during the PHE response in the presence or absence of LY (Fig. 7A,B). PHE also had little influence on Ser273 and Ser302 phosphorylation in the presence of calA (Supp Figure 1B). Taken together, low dose PHE does not uniformly increase phosphorylation levels at specific sites on these myofilament proteins, although there is evidence PHE accelerates phosphorylation turnover, at least at some sites (cTnISer23/24 and cMyBP-CSer282). While accelerated

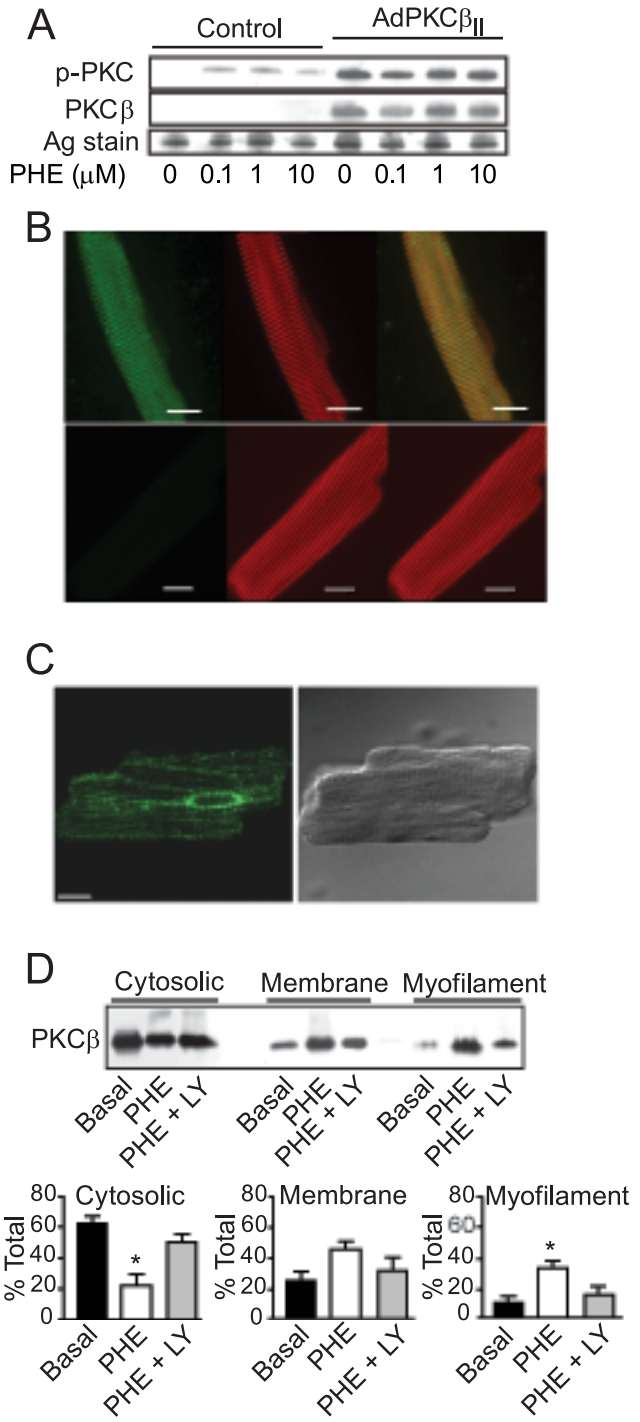

Figure 4 | Western and immunohistochemical analysis of PKCβ phosphorylation, localization and translocation in response to PHE. (A). Representative classical PKC isoform phosphorylation in response to 0.1–10 μM PHE in control and $PKC\beta_{II}$-expressing myocytes. The PHE-induced increases in phospho-PKC in control myocytes (left side), which do not express detectable $PKC\beta_{II}$ protein are observed because the phospho-antibody also detects PKCα phosphorylation. Raw blots for this panel are available in supplemental Figure 2. (B). Confocal projection image of PKCβ localization in response to 10 min of PHE (100 nM). $PKC\beta_{II}$-expressing (upper panel) and control (lower panel) myocytes were immunostained to detect PKCβ with FITC (left panels) and α-actinin with Texas Red (middle panels). Merged images in the far right panels show a similar striated distribution of PKCβ and α-actinin in myocytes expressing $PKC\beta_{II}$ (bars = 10 μm). The punctate distribution of $PKC\beta_{II}$ in response to PHE also overlapped with NCX (results not shown), which is expressed in the t-tubules[18]. (C). Fluorescence image showing $PKC\beta_{II}$ localization in response to 100 nM PHE plus 30 nM LY maintained the perinuclear distribution observed under basal conditions (see[16]; scale bar = 5 μm). (D). Representative fractionation (upper panel) and quantitative analysis (lower panel) of $PKC\beta_{II}$ distribution measured under basal conditions and in response to PHE or PHE+LY after fractionation. In these experiments, $PKC\beta_{II}$ is re-distributed from the cytosol to the myofilament fraction in response to low dose PHE, and this shift is blocked by LY. Results in the lower panel are expressed as mean±SEM (n = 7) and analyzed by one-way ANOVA and post-hoc Newman-Keuls comparisons, with significance set at $p < 0.05$ (*).

phosphorylation turnover in these myofilament proteins may not directly explain the maintenance of shortening during the PHE response in $PKC\beta_{II}$-expressing myocytes (Fig. 2), this observation also suggests it may be difficult to capture changes in phosphorylation level during an agonist response.

To determine whether a similar pattern of phosphorylation turnover develops in potential Ca^{2+} cycling targets, our focus turned to phospholamban (PLB) which can be phosphorylated at Ser16 and Thr17 (Fig. 8A,B). Low dose PHE tended to decrease PLB Ser16 phosphorylation (pSer16) in all 3 groups relative to the basal values[16]. The greatest decrease in PLB phosphorylation developed in $PKC\beta_{II}$-expressing myocytes, although this reduction was not significantly different from controls treated with PHE (Fig. 8A,B) and disappeared at higher PHE concentrations (Supp Fig. 1C). In contrast, PLB Thr17 phosphorylation (pThr17, Fig. 8A) was similar to controls and PKCβDN-expressing myocytes after treatment with PHE. Phosphorylation of this residue remained comparable to basal values[16] in controls and PKCβDN-expressing myocytes treated with PHE, while $PKC\beta_{II}$ reduced basal PLB Thr17 phosphorylation compared to controls. Thus, PHE increased PLB Thr17 phosphorylation in $PKC\beta_{II}$-expressing myocytes, such that these levels were comparable to controls. Addition of calA with PHE heightened phosphorylation of PLB pSer16 and pThr17 in all groups, although $PKC\beta_{II}$-expressing myocytes developed the most dramatic increases (Fig. 8A,B). PHE-mediated phosphorylation of these PLB residues in $PKC\beta_{II}$-expressing myocytes is similar to controls in the presence of LY (Fig. 8C).

Discussion

Our results show $PKC\beta_{II}$ up-regulation improves cardiac myocyte contractile function relative to controls in response to low dose PHE (Figs. 1,2). The same level of $PKC\beta_{II}$ up-regulation diminished basal contractile function in earlier work[16]. This ability of $PKC\beta_{II}$ to differentially modulate contractile function is consistent with the anticipated role of PKCs to act as a cellular mini-processor[17]. Spatial distribution appears to be one component of this processor, as diminished basal function correlates with peri-nuclear $PKC\beta_{II}$ localization[16], while a striated distribution pattern coincides with the PHE-induced response (Fig. 4). Based on our results, downstream kinase and phosphatase activation (Fig. 5[16],) and accelerated phosphorylation turnover in multiple end-target proteins (Figs. 6–8) also contribute to the $PKC\beta_{II}$ signaling processor. Further work is now needed to evaluate the level of accelerated phosphorylation turnover in myofilament and Ca^{2+} cycling end-target proteins after $PKC\beta_{II}$ up-regulation and identify whether multiple downstream kinases and phosphatases contribute to turnover on end targets.

Our results and earlier work show functional responses produced following classical PKC up-regulation are explained by changes in Ca^{2+} cycling and/or myofilament protein phosphorylation[10,16]. The increased PKCβ phosphorylation (Fig. 4) associated with the reduced shortening response to low dose PHE in control myocytes (Figs. 1,2) is consistent with the stimulation of protein phosphatase 1 (PP1) by this PKC isoform, which acts to decrease downstream PLB

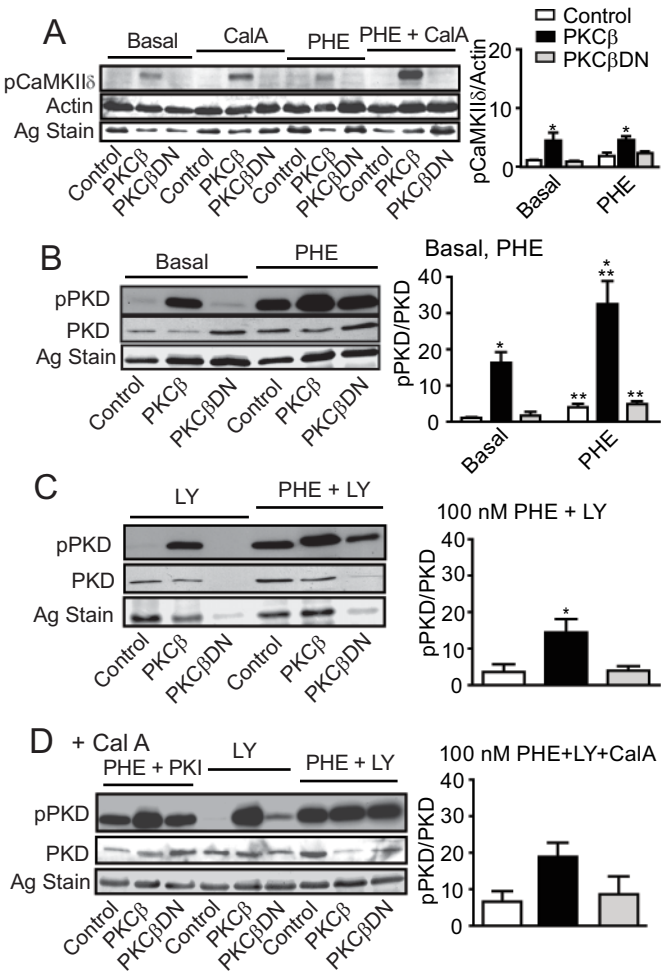

Figure 5 | CaMKIIδ phosphorylation (A) and PKD expression and phosphorylation (B, C) in adult rat myocytes treated with PHE. (A). Representative Western blot showing CaMKIIδ phosphorylation (pCaMKIIδ) under basal conditions and in response to 100 nM PHE (10 min) in the presence and absence of the phosphatase inhibitor, calyculin A (10 nM, calA). Quantitative analysis of basal and PHE-related CaMKIIδ phosphorylation in the absence of calA is shown in the right panel (Basal n = 8/group; PHE n = 3/group). Statistical comparisons were carried out using a 1-way ANOVA and post-hoc Newman-Keuls tests, with (*) $p < 0.05$ considered significantly different from control (right panel). This blot also shows the same lanes after membranes were re-probed for actin and the gels were silver (Ag)-stained to demonstrate protein loading in each lane. (B). Representative Western blot of phosphorylated PKD (pPKD), PKD and a silver- (Ag) stained portion of the same gel under basal conditions and in response to PHE (10 min, 100 nM PHE). A 2-way ANOVA and Newman-Keuls post-hoc tests are used to analyze the quantitative results shown in the right panel. A $p < 0.05$ is considered significantly different from control for comparisons among PKC groups (*) and for comparison to basal for groups treated with PHE (**; n = 5–6/group). There are no significant interaction effects. (C). Representative Western blot showing pPKD, PKD, and an Ag-stained portion of the gel in response to LY (30 nM) and PHE plus LY (10 min). The elevated pPKD observed under basal conditions continues to be observed during the PHE+LY response based on one-way ANOVA and Newman-Keuls post-hoc tests, with $p < 0.05$ (*) considered significantly different (n = 4/group). (D). Representative Western blot showing detection of pPKD, PKD and silver stained portion of the gel in response to PHE plus PKI, LY, and PHE + LY in the presence of calA. Quantitative analysis of the PHE + LY response in the presence of calA is shown in the right panel (n = 6/group) and compared using a 1-way ANOVA ($p > 0.05$). Raw blots and gel images for panels B and D are available in Supplemental Figure 2.

Ser16 phosphorylation[10]. The maintenance of contractile function in response to low dose PHE in myocytes expressing $PKC\beta_{II}$ activation (Figs. 1,2) also is associated with evidence showing both myofilament and Ca^{2+} cycling protein phosphorylation are targets for this isoform (Figs. 6–8). In our earlier work, $PKC\beta_{II}$ decreased contractile function and targeted the same proteins under basal conditions, and yet only the decrease in PLB Thr17 phosphorylation changed in a direction that could explain the diminished contractile function[16]. The restoration of PLB Thr17 phosphorylation toward basal control levels during the 100 nM PHE response (Fig. 8[16],) is consistent with this target working to maintain shortening amplitude (Fig. 1,2). However, experiments with calA demonstrate $PKC\beta_{II}$ expression is associated with a consistent acceleration of phosphorylation turnover in multiple myofilament and Ca^{2+} cycling proteins during the 100 nM PHE response (Figs. 6–8). While the phosphorylation state of a single residue, such as Thr17-PLB correlates with basal and PHE-induced changes in contractile function, the accelerated phosphorylation turnover may be the more important observation. Enhanced phosphorylation turnover could be an essential component of $PKC\beta_{II}$ signaling, by allowing small changes in the cellular microenvironment to rapidly modulate cardiac performance via shifts in the balance between kinase and phosphatase activity produced by $PKC\beta_{II}$. The increased PKD phosphorylation (Fig. 5) and differences in end target phosphorylation observed with and without the phosphatase inhibitor (Figs. 6–8) provide initial evidence to support the idea of bifurcated activation of kinases and phosphatases by $PKC\beta_{II}$. Parallel kinase and phosphatase activation also is consistent with complex patterns of target protein phosphorylation, as reported for basal[16] and agonist-stimulated conditions (Figs. 6–8).

Stochastic computational models are often used to explain similar behavior in other signaling and enzyme pathways[23–25]. Bi- or multistable models predict bifurcated signaling as well as external noise amplification[23,25]. Most importantly, models incorporating increased downstream kinase and phosphatase activity predict there are conditions when phosphorylation turnover is greatly enhanced, with little detected change in end-target phosphorylation. Thus, detected changes in target protein phosphorylation depend on large changes in phosphatase and/or kinase activity. The addition of a phosphatase inhibitor should dramatically influence end-target phosphorylation, which is clearly apparent in the response of $PKC\beta_{II}$-expressing myocytes to low dose PHE (Figs. 6–8). Based on these results, a stochastic model utilizing parallel activation of downstream kinases and phosphatases[23] is predicted to provide insight into $PKC\beta_{II}$ miniprocessor function and downstream function in cardiac myocytes in future work.

One important prediction from this type of model is that $PKC\beta_{II}$ up-regulation stimulates ATP and energy utilization in an effort to modulate contractile function. In cardiac myocytes, this up-regulation of $PKC\beta_{II}$ may be beneficial for modulating cardiac performance during early, compensated cardiac dysfunction. The initial $PKC\beta_{II}$ up-regulation may increase contractile performance if phosphorylation turnover is accelerated in response to low neurohormone levels. However, chronic up-regulation of this isoform could further tax hearts experiencing cellular stress, and ultimately cause deterioration in myocardial energetics and impair pump performance.

Stochastic modeling also could provide insight into the seemingly paradoxical relationship between cardiac dysfunction and PKCβ up-regulation reported in earlier work. $PKC\beta_{II}$ up-regulation is consistently reported during end-stage human heart failure[1,16,26] and in several animal models of heart failure[4,27]. Diminished cardiac performance develops in transgenic mice expressing wildtype $PKC\beta_{II}$[3,15], and yet inducible expression of constitutively active $PKC\beta_{II}$ enhances adult myocardium contractile function[12]. Enhanced phosphorylation turnover may develop in both mouse models, with downstream phosphatase activation favored in mice

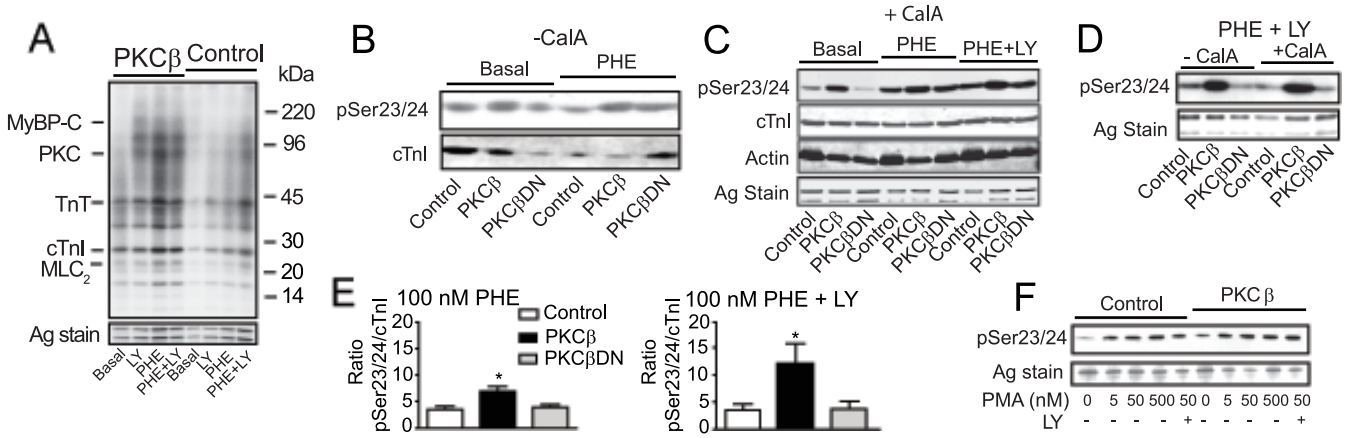

Figure 6 | Phosphorimage analysis (A) and Western blot analysis of cTnI Ser23/24 phosphorylation (pSer23/24) relative to total cTnI expression in response to PHE and PHE+LY (B–E). (A). Representative phosphorimage showing ^{32}P protein incorporation under basal conditions, and in response to LY (30 nM), PHE (100 nM) or PHE+LY for control and PKC-β_{II} expressing myocytes 2 days after gene transfer. Known phosphorylatable proteins are shown on the left side and molecular weight markers on the right. Proteins are separated with 12% SDS-PAGE prior to determining phosphate incorporation with a BioRad Phosphorimager. (B). Representative Western blot of cTnI pSer23/24 phosphorylation relative to cTnI expression in control, PKCβ- and PKCβDN-expressing myocytes under basal conditions and in response to 10 min of PHE (100 nM; 37°C). Experiments were carried out in the absence of calA. These results demonstrate PHE resulted in little change in cTnI pSer23/24 phosphorylation in the absence of phosphatase inhibitor. (C). Representative Western blot of cTnI pSer23/24 phosphorylation and cTnI in control, PKCβ- and PKCβDN-expressing myocytes under basal conditions and in response to 10 min of PHE (100 nM; 37°C) or PHE+LY in the presence of calA. Raw blots and gel images for this panel are available in Supplemental Figure 2. (D). Representative Western blot showing cTnI pSer23/24 and cTnI in controls and myocytes expressing PKCβ_{II} and PKCβDN treated with PHE and LY for 10 min in the absence (left) and presence (right) of calA. (E). Quantitative analysis of cTnI pSer23/24 phosphorylation relative to cTnI expression in response to PHE or PHE plus LY in the presence of calA. A 1-way ANOVA and post-hoc Newman-Keuls tests showed significant differences (* $p < 0.05$) when comparing phosphorylation in myocytes expressing PKCβ_{II}- compared to PKCβDN-expressing or control myocytes during the PHE (left panel; n = 3/group) and PHE+LY (right panel; n = 7/group) responses. The relative increase in cTnI pSer23/24 with PHE treatment detected in myocytes expressing PKCβ_{II} versus controls is comparable to the enhanced phosphorylation detected in the presence of calA under basal conditions[16]. (F). Representative Western analysis of cTnI pSer23/24 relative to a silver-stained portion of the gel in response to PMA (5–500 nM) in the absence and presence of LY. Phosphorylation of cTnI Ser23/24 is comparable in control and PKCβ_{II}-expressing myocytes.

expressing wildtype PKCβ_{II} and a tilt toward downstream kinase activity in mice expressing the constitutively active PKCβ_{II}.

Discrepancies among genetic as well as other PKCβ_{II}-related animal models and pre-clinical studies with the PKCβ inhibitor, ruboxistaurin indicate a model is needed to guide future work on PKCβ_{II} signaling in myocytes. For example, a PKCβ_{II}-specific inhibitor peptide proved to be functionally beneficial during chronic pressure overload in Dahl salt-sensitive rats[28], while activated PKCβ_{II} was functionally protective in an ischemia reperfusion injury model[29]. Other investigators using knockout mice also concluded PKCβ provides a modest protective effect against pressure overload[14]. In contrast, ruboxistaurin treatment of animal models developing heart failure reduced PKCβ expression and improved *in vivo* cardiac function[11,27]. Recently, these cardiac performance improvements were attributed to inhibition of PKCα rather than PKCβ[14]. However, the anticipated changes in downstream phosphorylation of end-target proteins which modulate contractile function and are targeted for phosphorylation by PKCα or β were not changed by ruboxistaurin treatment[30]. Future models are needed to explain these seemingly divergent results and the inability to capture changes in downstream target phosphorylation. A stochastic model incorporating the enhanced phosphorylation turnover detected here is a logical starting point.

Potential factors requiring further consideration in a future model include PKCβ_{II} localization and identification of alternative end targets. Our work shows PKCβ modulates myofilament, Ca^{2+} cycling,

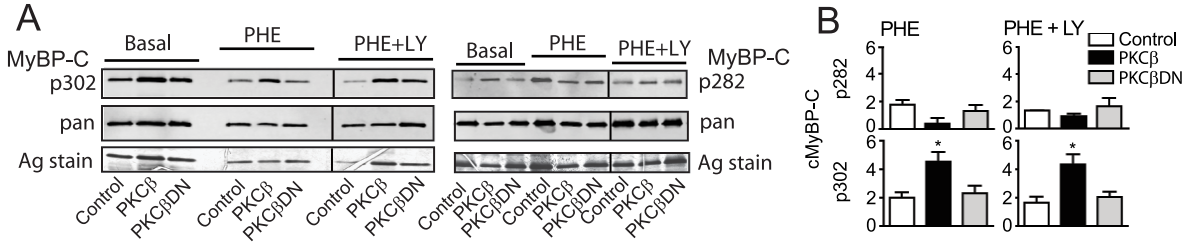

Figure 7 | Western blot (A) and quantitative (B) analyses of cardiac myosin binding protein C (cMyBP-C) phosphorylation in response to PHE (100 nM) in the presence and absence of LY. (A). Representative Western blots showing cMyBP-C phosphorylation at residues Ser302 (pSer302; left panel) and Ser282 (pSer282; right panel) relative to total cMyBP-C expression and a Ag-stained portion of each gel under basal, PHE-activated (100 nM; 10 min) and PHE+LY (10 min) treatments in controls, and myocytes expressing PKCβ_{II} and PKCβDN. Solid lines within each blot indicate a separation of samples on the same blot. Raw blot and gel images for basal and PHE treatments in this panel are available in Supplemental Figure 3. Phosphorylated Ser273 is not detected in these experiments (results not shown) and calA is not present in these experiments and in the quantitative analysis shown in panel B. (B). Quantitative analysis of pSer282 and pSer302 levels relative to total cMyBP-C detected with the pan Ab in response to PHE (left panel; n = 4/group) and PHE+LY (right panel; n = 4/group). A 1-way ANOVA and post-hoc Newman-Keuls tests (* $p < 0.05$) showed pSer302 phosphorylation is significantly elevated in PKCβ_{II}-expressing myocytes compared to values in control and PKCβDN-expressing myocytes.

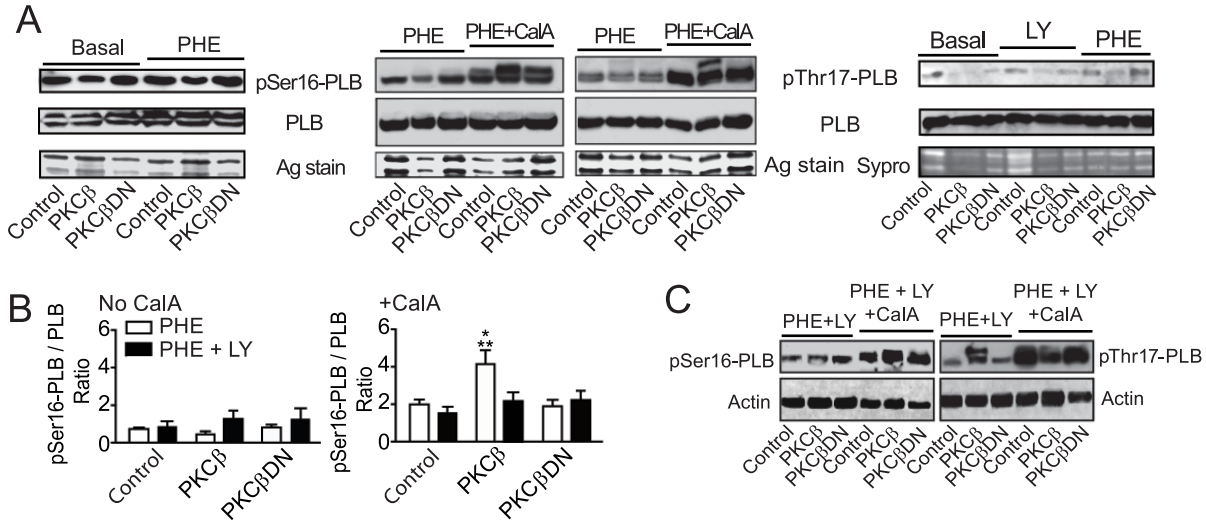

Figure 8 | Western blot and quantitative analyses of phospholamban (PLB) Ser16 and Thr17 phosphorylation in response to PHE in the presence and absence of LY. (A). Representative Western detection of pSer16-PLB (left panels) and pThr17-PLB (right panels) relative to total PLB under basal conditions and in response to PHE (100 nM, 10 min) or PHE plus calA in controls and myocytes expressing $PKC\beta_{II}$ or PKCβDN. Raw blot and gel images for PHE and PHE+CalA are available in Supplemental Figure 3. (B). Quantitative analyses of pSer16-PLB levels relative to total PLB in response to PHE and PHE+LY) in the absence (PHE n = 4–5/group; PHE+LY n = 3/group) and presence of calA (PHE n = 5/group; PHE+LY n = 4/group). Myocytes expressing $PKC\beta_{II}$ are compared to PKCβDN and controls using a 2-way ANOVA and post-hoc Newman-Keuls tests, with $p < 0.05$ (*, **) considered significant. Statistical comparisons were performed among the PKC group (*; control, $PKC\beta_{II}$ and PKCβDN) and among treatment groups (PHE vs PHE+LY; **) in the absence (left panel) and presence (right panel) of calA. (C). Representative pSer16-PLB and pThr17-PLB levels in response to PHE plus LY relative to actin. Experiments were performed with and without calA in controls and myocytes expressing $PKC\beta_{II}$ and PKCβDN. Quantitative results and the statistical comparisons are shown in panel B.

and kinase phosphorylation. In addition, there is evidence $PKC\beta_{II}$ may target CaMKII (Fig. 5A, ref. 31), phospholemman[32], ryanodine receptor[33], other cTnI residues[34,35], Cav1.5, and NCX[36]. The current results also show dramatic $PKC\beta_{II}$ localization changes in response to low dose PHE (Fig. 4) compared to the basal state[16]. Both $PKC\beta_{II}$ trafficking and the possibility this isoform accelerates phosphorylation turnover in additional protein targets will need to be factored into future models.

In summary, our work shows $PKC\beta_{II}$ signaling negatively modulates contractile function under basal conditions and positively modulates this function in response to a low dose α-adrenergic agonist. Complex patterns of downstream target phosphorylation are associated with both basal and agonist-stimulated conditions. Testable models are needed to understand the relationship between the contractile function and end target phosphorylation responses. A stochastic model incorporating bifurcated signaling is discussed as a starting point for this work based on our current observations. Additional elements to explain $PKC\beta_{II}$ modulation of contractile function are likely to include alternative targets, trafficking, PKC isoform dominance, as well as PKC isoform feedback loops[17]. Future computational models are anticipated to provide insight into the $PKC\beta_{II}$ signaling pathway and pave the way for pre-clinical therapies.

Methods

Myocyte isolation and gene transfer. Adult rat cardiac myocytes were isolated, made Ca^{2+}-tolerant, and plated on laminin-coated coverslips in DMEM plus 5% FBS, penicillin (50 U/ml) and streptomycin (50 μg/ml; P/S) for 2 hours, as described earlier[16,37]. Gene transfer of $PKC\beta_{II}$ or PKCβDN was carried out in serum-free DMEM plus P/S using recombinant adenoviral vectors (10 MOI)[37] for 1 hr followed by the addition of M199 plus P/S media. Electrical pacing of myocytes was initiated 24 hrs after plating in M199 media plus P/S, with media changes every 12 hrs[37]. Experiments with myocytes were performed 2 days after gene transfer unless otherwise noted. All animal procedures utilized for these studies followed the guidelines of and were approved by the University Committee on Use and Care of Animals at the University of Michigan.

Contractile function measurements. Sarcomere shortening in isolated myocytes was measured with a video-based microscope platform (Ionoptix, Beverly, MA) in a 37°C temperature-controlled chamber perfused with M199 with or without agonist[38,39]. Resting sarcomere length, peak shortening amplitude, shortening and re-lengthening rates (μm/sec), time to peak (TTP), plus times to 25%, 50%, and 75% re-lengthening ($TTR_{25\%}$, $TTR_{50\%}$, $TTR_{75\%}$) were measured from signal averaged recordings of myocytes. Contractile function was measured under basal conditions and in response to the α_1 agonist, phenylephrine (PHE; 0.1 and 1 μM), and to PMA (50 nM). The contribution of $PKC\beta_{II}$ to the PHE response was evaluated with and without the PKCβ inhibitor, LY379196 (LY; 30 nM; kind gift of Dr. Chris Vlahos, Eli Lilly)[40,41].

Western analysis. Expression and phosphorylation of PKCβ also were measured in myocytes 2 days after gene transfer. Myocytes were collected into sample buffer, proteins were separated using 12% SDS-PAGE, and then transferred onto PVDF membrane for all proteins studied, as described earlier[16,37,38]. $PKC\beta_{II}$ expression and phosphorylation levels were detected by Western analysis using enhanced chemiluminesence. For Western detection, membranes were incubated in primary antibodies directed to $PKC\beta_{II}$ (BD Biosciences, San Jose, CA) or phosphorylated PKCα/β (Cell Signaling Technology, Danvers, MA) followed by horseradish peroxidase-conjugated secondary antibodies and detected with film. Expression and phosphorylation of downstream targets also were analyzed by Western analysis. Primary antibodies directed to phospho-cTnISer23/24 (Cell Signaling), troponin I (Millipore), phospholamban (PLB), phosphoSer16-PLB (pSer16-PLB), phosphoThr17-PLB (pThr17-PLB), as well as expression and phosphorylation of cardiac myosin binding protein C (cMyBP-C), phospho-Ser273-, phospho-Ser282-, and phospho-Ser302- cMyBP-C, Ca^{2+}-calmodulin-dependent protein kinase IIδ (CAMKIIδ), and protein kinase D (PKD) were utilized and detected as described in detail in earlier work[16]. After detection of phosphorylated PKCβ, troponin I, PLB, cMyBP-C, CamKIIδ, and PKD, membranes were stripped and re-probed for total expression of the same protein with the exception of CamKIIδ, which was probed for actin. Films were scanned using a scanner (Microtek ScanMaker 4) with the resolution set at 600 dpi. Quantitative analysis of protein expression was carried out with Quantity One software and normalized to total expression of the same protein or actin.

Indirect immunofluorescence imaging. PKCβ localization in myocytes was determined by immunohistochemical staining of paraformaldehyde-fixed cells[16,38]. Cellular distribution of PKCβ was determined using the same primary $PKC\beta_{II}$ antibody described under protein detection and a goat anti-mouse secondary antibody conjugated to fluorescein isothiocyanate (FITC, Invitrogen). The PKCβ distribution in response to 10 min PHE (100 nM), or 10 min PHE plus LY379196 (30 nM) was analyzed in control and $PKC\beta_{II}$-expressing myocytes. In a subset of myocytes, dual immunostaining with the PKCβ antibody and α-actinin antibody

(EA-53; 1 : 500) was performed to determine whether PKCβ$_{II}$ is distributed in a striated pattern similar to the myofilament z-band in response to 100 nM PHE (10 min). Primary antibody binding was detected with secondary antibodies conjugated to FITC- and Texas Red (TR), respectively. Myocytes immunostained for α-actinin and PKCβ after treatment with PHE were imaged using a Fluoview 500 laser scanning confocal microscope (Olympus) without deconvolution. Images collected after treatment with PHE plus LY379196 were obtained with a Nikon Ti-U fluorescence microscope.

Fractionation studies. Cells were fractionated after a 10 min treatment under basal conditions in M199 containing the phosphatase inhibitor, calA (10 nM), or in M199 plus calA containing 100 nM PHE with or without 30 nM LY at 37°C. Then, myocytes were collected in ice-cold lysis buffer (20 mM Tris, pH 7.5, 2 mM EDTA, 2 mM EGTA, 250 mM sucrose, 6 mM β-mercaptoethanol, 48 μg/ml leupeptin, 5 μM pepstatin, 0.1 mM Na orthovanadate, and 50 mM NaF) and centrifuged at 1000 × *g* for 10 min at 4°C, as described earlier[19,42]. The supernatant was further fractionated for 1 hr at 100,000 × *g* into a cytosol-enriched supernatant, and non-nuclear membrane enriched pellet[19,42]. Ice cold sample buffer was added to each sub-fraction, then briefly sonicated, and then proteins separated on 12% SDS-PAGE gels, transferred to PVDF membranes, and analyzed for PKCβ$_{II}$ expression.

Radiolabeling studies. Phosphorylation of downstream targets in response to 10 min PHE (100 nM) with and without LY (30 nM) was initially analyzed in radiolabeled myocytes[43]. Myocytes labeled with ^{32}P-orthophosphate (100 μCi) for 2 hrs at 37°C were transferred to un-labeled M199 media containing 10 nM calA (basal), or the same media with PHE (0.1 μM) with and without LY (30 nM) for 10 min. Phosphorylation was terminated in ice-cold relaxing solution (RS; 7 mM EGTA, 20 mM imidazole, 1 mM free Mg^{2+}, 14.5 mM creatine phosphate, and 4 mM MgATP with KCl added to yield an ionic strength of 180 mM, pH 7.00) and myocytes were collected into ice-cold sample buffer[16]. Proteins in each sample are separated on a 12% SDS-PAGE gel, and then the silver- (Ag) stained gel was dried overnight. Phosphorylation was analyzed using a Phosphor-imager (Bio-Rad, Hercules, CA), and radioactive bands were quantified after an overnight cassette exposure using Quantity One software (Bio-Rad, Hercules, CA). Contractile proteins were identified based on their migration relative to mw markers.

Statistical analysis. Quantitative results are expressed as mean ± SEM, and an unpaired Student's t-test or one-way analysis of variance (ANOVA) and post-hoc Newman-Keuls tests are used to analyze myocyte contractile function. Quantitative analysis of protein expression and phosphorylation levels are compared using a one- or two-way ANOVA and post-hoc Newman-Keuls tests, with $p < 0.05$ considered statistically significant. Measurements of PKCβ$_{II}$ expression and ^{32}P-labeled phosphor-images in fractionated myocytes are normalized to SDS-PAGE Ag-stained gels and values are expressed relative to controls.

1. Bowling, N., Walsh, R. A., Song, G. J., Estridge, T., Sandusky, G. E., Fouts, R. L., Mintze, K., Pickard, T., Roden, R., Bristow, M. R., Sabbah, H. N., Mizrahi, J. L., Gromo, G., King, G. L. & Vlahos, C. J. Increased protein kinase C activity and expression of Ca2+-sensitive isoforms in the failing human heart. *Circulation* **99**, 384–391 (1999).
2. Bowman, J. C., Steinberg, S. F., Jiang, T. R., Geenen, D. L., Fishman, G. I. & Buttrick, P. M. Expression of protein kinase C beta in the heart causes hypertrophy in adult mice and sudden death in neonates. *J Clin Invest* **100**, 2189–2195 (1997).
3. Takeishi, Y., Chu, G. X., Kirkpatrick, D. M., Li, Z. L., Wakasaki, H., Kranias, E. G., King, G. L. & Walsh, R. A. In vivo phosphorylation of cardiac troponin I by protein kinase C β2 decreases cardiomyocyte calcium responsiveness and contractility in transgenic mouse hearts. *J Clin Invest* **102**, 72–78 (1998).
4. Gu, X. & Bishop, S. P. Increased Protein-Kinase-C and Isozyme Redistribution in Pressure-Overload Cardiac-Hypertrophy in the Rat. *Circ Res* **75**, 926–931 (1994).
5. Hambleton, M., Hahn, H., Pleger, S. T., Kuhn, M. C., Klevitsky, R., Carr, A. N., Kimball, T. F., Hewett, T. E., Dorn, G. W. 2nd, Koch, W. J. & Molkentin, J. D. Pharmacological- and gene therapy-based inhibition of protein kinase Calpha/beta enhances cardiac contractility and attenuates heart failure. *Circulation* **114**, 574–582 (2006).
6. Koide, Y., Tamura, K., Suzuki, A., Kitamura, K., Yokoyama, K., Hashimoto, T., Hirawa, N., Kihara, M., Ohno, S. & Umemura, S. Differential induction of protein kinase C isoforms at the cardiac hypertrophy stage and congestive heart failure stage in Dahl salt-sensitive rats. *Hypertension Res* **26**, 421–426 (2003).
7. Liu, Q. & Molkentin, J. D. Protein kinase Cα as a heart failure therapeutic target. *J Mol Cell Cardiol* **51**(**4**), 474–478 (2011).
8. Rybin, V. & Steinberg, S. F. Do adult rat ventricular myocytes express protein kinase C alpha? *Am J Physiol Heart Circ Physiol* **272**, H2485–H2491 (1997).
9. Steinberg, S. F., Goldberg, M. & Rybin, V. O. Protein kinase C isoform diversity in the heart. *J Mol Cell Cardiol* **27**, 141–153 (1995).
10. Braz, J. C., Gregory, K., Pathak, A., Zhao, W., Sahin, B., Klevitsky, R., Kimball, T. F., Lorenz, J. N., Nairn, A. C., Liggett, S. B., Bodi, I., Wang, S., Schwartz, A., Lakatta, E. G., DePaoli-Roach, A. A., Robbins, J., Hewett, T. E., Bibb, J. A., Westfall, M. V., Kranias, E. G. & Molkentin, J. D. PKC-α regulates cardiac contractility and propensity toward heart failure. *Nat Med* **10**, 248–254 (2004).
11. Connelly, K. A., Kelly, D. J., Zhang, Y., Prior, D. L., Advani, A., Cox, A. J., Thai, K., Crum, H. & Gilbert, J. E. Inhibition of protein kinase C-β by ruboxistaurin preserves cardiac function and reduces extracellular matrix production in diabetic cardiomyopathy. *Cir Heart Fail* **2**, 129–137 (2009).
12. Huang, L., Wolska, B. M., Montgomery, D. E., Burkart, E. M., Buttrick, P. M. & Solaro, R. J. Increased contractility and altered Ca^{2+} transients of mouse heart myocytes conditionally expressing PKCβ. *Am J Physiol Cell Physiol* **280**, C1114–C1120 (2001).
13. Kariya, K., Karns, L. R. & Simpson, P. C. Expression of A Constitutively Activated Mutant of the Beta-Isozyme of Protein-Kinase-C in Cardiac Myocytes Stimulates the Promoter of the Beta-Myosin Heavy-Chain Isogene. *J Biol Chem* **266**, 10023–10026 (1991).
14. Liu, Q., Chen, X., MacDonnell, S. M., Kranias, E. G., Lorenz, J. N., Leitges, M., Houser, S. R. & Molkentin, J. D. Protein kinase Cα, but not PKCβ or PKCy Regulates Contractility and Heart failure susceptibility. *Circ Res* **105**, 194–200 (2009).
15. Wakasaki, H., Koya, D., Schoen, F. J., Jirousek, M. R., Ways, D. K., Hoit, B. D., Walsh, R. A. & King, G. I. Targeted overexpression of protein kinase C β2 isoform in myocardium causes cardiomyopathy. *Proc Nat Acad Sci* **94**, 9320–9325 (1997).
16. Hwang, H., Robinson, D. A., Stevenson, T. K., Wu, H. C., Kampert, S. E., Pagani, F. D., Dyke, D. B., Martin, J. L., Sadayappan, S., Day, S. M. & Westfall, M. V. PKCβ(II) modulation of myocyte contractile performance. *J Mol Cell Cardiol* 14 May 2012. [Epub ahead of print] PMID: 22587992.
17. Steinberg, S. F. Structural basis of protein kinase C isoform function. *Physiol Rev* **88**, 1341–1378 (2008).
18. Thomas, M. J., Sjaastad, I., Andersen, K., Helm, P. J., Wasserstrom, J. A., Sejersted, O. M. & Ottersen, O. P. Localization and function of the Na^+/Ca^{2+}-exchanger in normal and detubulated rat cardiomyocytes. *J Mol Cell Cardiol* **35**, 1325–1337 (2003).
19. Jonjev, Z. S., Schwertz, D. W., Beck, J. M., Ross, J. D. & Law, W. D. Subcellular distribution of protein kinase C isozymes during cardioplegic arrest. *J Thorc Cardiovasc Surg* **126**,1880–1885 (2003).
20. Haworth, R. S., Cuello, F. & Avkiran, M. Regulation of phosphodiesterase isoforms of protein kinase A-mediated attenuation of myocardial protein kinase D activation. *Basic Res Cardiol* **106**, 51–63 (2010).
21. Bardswell, S. C., Cuello, F., Rowland, A. J., Sadayappan, S., Robbins, J., Gautel, M., Walker, J. W., Kentish, J. C. & Avkiran, M. Distinct sarcomeric substrates are responsible for protein kinase D-mediated regulation of cardiac myofilament Ca^{2+}-sensitivity and cross-bridge cycling. *J Biol Chem* **285**, 5674–5682 (2010).
22. Xiao, L., Zhao, Q., Du, Y., Yuan, C., Solaro, R. J. & Buttrick, P. M. PKCepsilon increases phosphorylation of the cardiac myosin binding protein C at serine 302 both in vitro and in vivo. *Biochemistry* **46**, 7054–7061 (2007).
23. Bishop, L. M. & Qian, H. Stochastic bistability and bifurcation in a mesoscopic signaling system with autocatalytic kinase. *Biophys J* **90**, 1–11 (2010).
24. Chaudhri, V. K., Kumar, D., Misra, M., Dua, R. & Rao, K. V. S. Integration of a phosphatase cascade with the mitogen-activated protein kinase pathway provides for a novel signal processing function. *J Biol Chem* **285**, 1296–1310 (2010).
25. Samilov, M., Plyasunov, S. & Arkin, A. P. Stochastic amplificaton and signaling in enzymatic futile cycles through noise -induced bistability with oscillations. *Proc Nat Acad Sci* **102**, 2310–2315 (2005).
26. Noguchi, T., Hunlich, M., Camp, P. C., Begin, K. J., El Zaru, M., Patten, R., Leavitt, B. J., Ittleman, F. P., Alpert, N. R., LeWinter, M. M. & Van Buren, P. Thin filament-based modulation of contractile performance in human heart failure. *Circulation* **110**, 982–987 (2004).
27. Liu, Y., Lei, S., Gao, X., Mao, X., Wang, T., Wong, G. T., Van Houtte, P. M., Irwin, M. G. & Xia, Z. PKCβ inhibition with ruboxistaurin reduces oxidative stress and attenuates left ventricular hypertrophy and dysfunction in rats with streptozotocin-induced diabtetes. *Clin Sci London* **122**, 161–173 (2012).
28. Ferriera, J. C. B., Koyanagi, T., Palaniyandi, S. S., Fajardo, G., Churchill, E. N., Budas, G., Disatnik, M.-H., Bernstein, D., Brum, P. C. & Mochly-Rosen, D. Pharmacological inhibition of βIIPKC is cardioprotective in late-stage hypertrophy. *J Mol Cell Cardiol* **51**, 980–987 (2011).
29. Tian, R., Miao, W., Spindler, M., Javadpour, M. M., McKinney, R., Bowman, J. C., Buttrick, P. M. & Ingwall, J. S. Long-term expression of protein kinase C in adult mouse hearts improves postischemic recovery. *Proc Natl Acad Sci* **96**, 13536–13541 (1999).
30. Ladage, D., Tilemann, L., Ishikawa, K., Correll, R. N., Kawase, Y., Houser, S. R., Molkentin, J. D. & Hajjar, R. J. Inhibition of PKCα/β with ruboxistaurin antagonizes heart failure in pigs after myocardial infarction injury. *Circ Res* **109**, 1396–1400 (2011).
31. Waxham, M. N. & Aronowski, J. Ca^{2+}/calmodulin-dependent protein kinase II is phosphorylated by protein kinase C in vitro. *Biochemistry* **32**, 2923–2930 (1993).
32. Han, F., Bossuyt, J., Despa, S., Tucker, A. L. & Bers, D. M. Phospholemman phosphorylation mediates protein kinase C-dependent effects on Na^+/K^+ pump function in cardiac myocytes. *Circ Res* **99**, 1376–1383 (2006).
33. Allen, B. G. & Katz, S. Phosphorylation of cardiac junctional and free sarcoplasmic reticulum by PKCα, PKCβ, PKA and the Ca^{2+}/calmodulin-dependent protein kinase. *Mol Cell Biochem* **155**, 91–103 (1996).
34. Kobayashi, T., Yang, X., Walker, L. A., Van Breemen, R. B. & Solaro, R. J. A non-equilibrium isoelectric focusing method to determine states of phosphorylation of cardiac troponin I: Identification of Ser-23 and Ser-24 as significant sites of phosphorylation by protein kinase C. *J Mol Cell Cardiol* **38**, 213–218 (2005).

35. Wang, H., Grant, J. E., Doede, C. M., Sadayappan, S., Robbins, J. & Walker, J. W. PKC-βII sensitizes cardiac myofilaments to Ca^{2+} by phosphorylating troponin I on threonine-144. *J Mol Cell Cardiol* **41**, 823–833 (2006).
36. Zhang, Y. H. & Hancox, J. C. Regulation of cardiac Na^{+}-Ca^{2+} exchanger activity by protein kinase phosphorylation – Still a paradox? *Cell Calcium* **45**, 1–10 (2009).
37. Westfall, M. V., Rust, E. M., Albayya, F. & Metzger, J. M. Adenovirus-mediated myofilament gene transfer into adult cardiac myocytes. *Methods Cell Biol* **52**, 307–322 (1997).
38. Green, J. J., Robinson, D. A., Wilson, G. E., Simpson, R. U. & Westfall, M. V. Calcitrioll modulation of cardic contractile performance via protein kinase C. *J Mol Cell Cardio.* **41**, 350–359 (2006).
39. Westfall, M. V., Lee, A. M. & Robinson, D. A. Differential contribution of troponin I phosphorylation sites to the endothelin-mediated contractile response. *J Biol Chem* **280**, 41324–31 (2005).
40. Jirousek, M. R., Gillig, J. R., Gonzalez, C. M., Heath, W. F., McDonald, J. H., Neel, D. A., Rito, C. J., Singh, U., Stramm, L. E., MelikianBadalian, A., Baevsky, M., Ballas, L. M., Hall, S. E., Winneroski, L. L. & Faul, M. M. (S)-13-[(dimethylamino)methyl]-10,11,14,15-tetrahydro-4,9 : 16,21-dimetheno-1H,13H-dibenzo[e,k]pyrrolo[3,4-h][1,4,13]oxadiazacyclohexadecene-1,3(2H)-dione (LY333531) and related analogues: Isozyme selective inhibitors of protein kinase C beta. *J Med Chem* **39**, 2664–2671 (1996).
41. Zhang, Y., Bloem, L. J., Yu, L., Estridge, T. B., Iversen, P. W., McDonald, C. E., Schrementi, J. P., Wang, X. & Vlahos, C. Protein kinase C betaII activation induces angiotensin converting enzyme expression in neonatal rat cardiomyocytes. *Cardiovasc Res* **57**, 139–46 (2003).
42. Reid, E. A., Kristo, G., Yoshimura, Y., Ballard-Croft, C., Keith, B. J., Mentzer, R. M. Jr. & Lasley, R. D. *In vivo* adenosine receptor preconditioning reduces myocardial infarct size via subcellular ERK signaling. *Am J Physiol Heart Circ Physiol* **288**, H2253–H2259 (2005).
43. Westfall, M. V. & Borton, A. R. Role of troponin I phosphorylation in protein kinase C-mediated enhanced contractile performance of rat myocytes. *J Biol Chem* **278**, 33694–33700 (2003).

Acknowledgements

Immunohistochemical imaging was carried out at The University of Michigan Morphology and Imaging core of the Michigan Diabetes Research and Training Center funded by NIH5P60 DK20572 from the National Institute of Diabetes & Digestive & Kidney Diseases. The technical assistance of Gail Romanchuk also is gratefully acknowledged. This work was supported by the National Institutes of Health (HL067254 and HL089093 to MVW).

Author contributions

H.H., D.R. and M.W. performed experiments, analyzed and discussed data shown Figures 1–3. Discussed data interpretation and reviewed the manuscript. H.H., J.R. and M.W. performed experiments, analyzed and discussed data for Figure 4. T.S. and M.W. performed experiments, analyzed and discussed data shown in Figures 5, 6 and 8. S.L. and M.W. performed experiments, analyzed and discussed data shown in Figure 7. S.a.S. and S.D. contributed reagents, discussed interpretation and reviewed the manuscript. S.i.S. and M.W. discussed data interpretation, wrote and reviewed the manuscript.

Additional information

Supplementary information accompanies this paper at http://www.nature.com/scientificreports

Competing financial interests: The authors declare no competing financial interests.

How to cite this article: Hwang, H. *et al.* Agonist Activated $PKC\beta_{II}$ Translocation and Modulation of Cardiac Myocyte Contractile Function. *Sci. Rep.* **3**, 1971; DOI:10.1038/srep01971 (2013).